Research article

National wetland mapping using remote-sensing-derived environmental variables, archive field data, and artificial intelligence

Sébastien Rapinel [a],[*], Léa Panhelleux [a], Guillaume Gayet [b], Rachel Vanacker [b], Blandine Lemercier [c], Bertrand Laroche [d], François Chambaud [e], Anis Guelmami [f], Laurence Hubert-Moy [a]

[a] LETG UMR 6554, University of Rennes - CNRS, place du recteur Henri le Moal, Rennes, 35000, France
[b] PatriNat OFB-CNRS-MNHN, 57 rue Cuvier, Paris, 75231, France
[c] SAS UMR 1069, Institut Agro Rennes-Angers - INRAE, 65 rue de Saint-Brieuc, Rennes, 35000, France
[d] InfoSol-US 1106, INRAE, Orléans, 45075, France
[e] Agence de l'eau Rhône Méditerranée Corse, 2-4 allée de Lodz, Lyon, 69363, France
[f] Tour du Valat, Le Sambuc, Arles, 13200, France

ARTICLE INFO

ABSTRACT

While wetland ecosystem services are widely recognized, the lack of fine-scale national inventories prevents successful implementation of conservation policies. Wetlands are difficult to map due to their complex fine-grained spatial pattern and fuzzy boundaries. However, the increasing amount of open high-spatial-resolution remote sensing data and accurately georeferenced field data archives, as well as progress in artificial intelligence (AI), provide opportunities for fine-scale national wetland mapping. The objective of this study was to map wetlands over mainland France (ca. 550,000 km^2) by applying AI to environmental variables derived from remote sensing and archive field data. A random forest model was calibrated using spatial cross-validation according to the precision-recall area under the curve (PR-AUC) index using ca. 135,000 soil or flora plots from archive databases, as well as 5 m topographical variables derived from an airborne DTM and a geological map. The model was validated using an experimentally designed sampling strategy with ca. 3000 plots collected during a ground survey in 2021 along non-wetland/wetland transects. Map accuracy was then compared to those of nine existing wetland maps with global, European, or national coverage. The model-derived suitability map (PR-AUC 0.76) highlights the gradual boundaries and fine-grained pattern of wetlands. The binary map is significantly more accurate (F1-score 0.75, overall accuracy 0.67) than existing wetland maps. The approach and end-results are of important value for spatial planning and environmental management since the high-resolution suitability and binary maps enable more targeted conservation measures to support biodiversity conservation, water resources maintenance, and carbon storage.

---

* Corresponding author.
  E-mail address: sebastien.rapinel@univ-rennes2.fr (S. Rapinel).

1. Introduction

Wetlands contribute to about 40% of the total value of ecosystem services [1] defined as benefits provided by natural systems that contribute to social welfare [2], such as food supply, biodiversity conservation, and flood regulation [1]. Although scientists, policy makers, and citizens widely recognize the benefits of wetland services, threats to these ecosystems have increased in recent decades [3–5]. Human activities such as urbanization and agriculture intensification are responsible for about 35% of wetland loss in natural wetlands since the 1970's at a global scale [3,6], and up to 45% in Europe [6], while artificial wetlands have increased by 233% [3]. Climate change also threatens wetlands as fresh water availability decreases and sea level rises [7,8], resulting respectively in an expected loss of 1% of Ramsar inland wetlands [9] and 20% of coastal wetlands in the future decades [10]. These increasing trends are partly due to the unavailability of reliable and comprehensive wetland maps, which limits implementation of conservation policies [11]. While internationally important wetlands have been widely mapped and monitored [3,12], most small and common wetlands are ignored in national maps [13]. Mapping these wetlands is critical due to their (i) complex fine-grained spatial pattern, (ii) scattered distribution, and (iii) fuzzy boundaries between terrestrial and aquatic ecosystems, which raise definitional issues [14,15]. Some national wetlands have been inventoried by using soil maps [16] or combining historical and geological maps [17], but the uncertainty in these data, which can be high, generates inaccuracy in wetland-prediction maps [18,19].

Remote sensing data, which provide continuous, comprehensive, and standardized observation of terrestrial ecosystems over large areas [20], have been widely used to map wetlands [21,22]. While providing broad coverage, they have often been used for local wetland inventories [23,24], since national inventories are conducted by compiling local wetland maps, as in the United States [25]. However, this latter approach is time-consuming and expensive [14], and results in a non-comprehensive map of inconsistent quality due to the multiple definitions, scales, and methods used to produce local wetland maps [13]. In a context of increasing dissemination of field or remote sensing data, growing computational resources, and progress in artificial intelligence (AI), the development of operational and standardized approaches has recently been promoted [23,24,26,27].

Based on this research trend, several recent national and international wetland inventories have used remote sensing data following two main approaches. The first approach identifies wetlands based on their vegetation type (e.g. bogs, fens, salt marshes, swamps, mangroves) and/or their flooding dynamics using optical [28] or radar [29] satellite time series from which vegetation, soil and water indices can be derived. This approach has been applied at spatial resolutions of ca. 8 km over the entire globe [30], 250 m over Myanmar [24], 30 m over China [31], 23 m over India [32], and up to 10 m over Canada [33] and Minnesota [34]. However, this approach has major disadvantages in that it cannot detect (i) water-saturated wetlands covered with vegetation similar to that on non-wetlands (e.g. grasslands, forests, heathlands, crops) [14,22], even though most wetlands in the world are of this type [35,36]; and (ii) damaged wetlands (e.g. now covered by crops or impervious surfaces) in which hydrological functions are nevertheless still effective [27,36,37].

The second approach avoids these disadvantages by identifying the maximum (i.e. potential) wetland extent based on topographic variables [26,38]. These variables can be derived from either satellite [39] or airborne [40] remote sensing data. This approach is particularly appropriate for supporting national mapping since it identifies most wetlands, including those covered by common types of vegetation or those that have been damaged and where restoration could be initiated [41]. This second approach was first applied at spatial resolutions of 1 km over Europe [42] and 50 m over France [43], and more recently 500 m over the entire globe [35], 30 m over Rwanda [44] and Albania [45], and up to 25 m over Europe [46]. These studies used mainly open-source digital terrain models (DTMs) derived from satellite data, however, which have two disadvantages for wetland inventories: (i) their decametric vertical accuracy is too low to capture micro-topography [47], which decreases the accuracy of wetland delineation, and (ii) their spatial resolution does not exceed 25 m, which limits detection of narrow or small wetlands [26]. Several studies have emphasized the need to use airborne DTMs with vertical accuracy of ca. 0.2 m and spatial resolution of 1–5 m to identify small wetlands, including those under forest cover [14,41,48–50]. These studies were conducted at the local scale and should be extended to the national scale, especially since open-access national airborne DTMs are increasingly available [41].

The consistency and accuracy of wetland mapping is a key issue for users [13]. To this end, reference field data are essential to calibrate and validate the models [26]. Large amounts of reference field data are required to model large areas, such as for national wetland inventories [33,51]. However, using a robust model to map wetlands at a national scale is challenging given the limited availability of reference data that cover an entire country [31,33]. For operational reasons, most national wetland inventories based on remote sensing data use pseudo reference field data, for example from local "field" maps derived from analyzing satellite or airborne images at very high spatial resolution, and/or directly from visually interpreting the latter [24,27,31–33,42,44,46]. While these pseudo reference field data may be acceptable to the remote sensing scientific community [52], they have higher uncertainty (due to mislabeling and lower polygon-contour accuracy) than real georeferenced field plots, which simultaneously decreases model accuracy [53] and provides over-optimistic estimates of it [54]. Furthermore, these pseudo reference field data frequently do not include damaged wetlands [27,44,46]. Thus, reference data obtained from field plots is preferred to visual interpretation of remote sensing images at very high spatial resolution [27], although collecting field data for an entire country is time-consuming and costly [14].

For a national wetland mapping, cost and operational criteria are as important as map accuracy [26]. Archive field databases appear to be an obvious resource for national wetland inventories because they are immediately available, free of charge, easily accessible, ready to use, and contain tens of thousands of accurately georeferenced field plots worldwide [51]. Soil and vegetation plots are particularly useful for spatial wetland modeling. Specifically, the use of soil plots enabled assessing the accuracy of the map of potential wetlands [38], including crops or urban areas, which have not been considered in national inventories [27,42,44,46]. Many vegetation databases, such as those of the Global Biodiversity Information Facility [55] and National Forest Inventory (NFI), have been successfully used for spatial modeling of natural vegetation [56]. Soil databases have been increasingly available in recent years,

especially via the GlobalSoilMap project [57]. These soil plots, numbering ca. 800,000 worldwide, have notably been used to develop national soil maps [18]. However, these archive databases of vegetation and soil surveys have not been used to map wetlands.

The model robustness is another challenge of using AI to map wetlands at national scale [33]. Besides being due to the properties of the training samples and the explanatory variables, model robustness may also be due to hyper-parametrization [56]. Specifically, two points received little attention in wetland modeling: (i) selection of an appropriate accuracy metric and (ii) addressing spatial auto-correlation [56]. Traditionally, a probabilistic model such as random forest (RF) is fitted using threshold-dependent metrics such as overall accuracy (OA) or the Kappa index. However, the default threshold of 0.5 is usually not optimal, which decreases model accuracy [58], conversely to threshold-independent metrics such as precision-recall area under the curve (PR-AUC) index, which are better suited to the model probabilistic output. Regarding spatial autocorrelation, many open-source tools provide simple features that limit it during cross-validation procedure [59].

Another issue in wetland mapping is to delineate clearly the boundaries between wetlands and non-wetlands [14]. Although the transition between aquatic and terrestrial environments varies in width [15,26], most wetland mapping studies report binary (i.e. "wetland" vs. "not wetland") model output directly [26]. Besides ignoring user expertise in the process [24], this approach raises two issues: (i) the land-water *continuum* is not highlighted and (ii) the threshold used to classify model output is rarely optimal [44,56]. However, these boundaries can be spatialized using model output of a continuous variable (i.e., confidence level) [60]. Considering the suitability map as the main product is interesting since it renders *continuum* between non-wetlands and wetlands spatially explicit [60]. The suitability map is more useful than a binary map when conflicts arise between users [61]. Moreover, the suitability map encourages map users to become involved since they can adapt thresholds based on their field expertise [24]. A binary wetland map can then be obtained by thresholding, which can be adapted to the ecological region and user needs [60].

The objective of this study was to map wetlands over mainland France (ca. 550,000 km^2) by applying AI to environmental variables derived from remote sensing and archive field data. Three research questions were addressed: (i) Are environmental variables derived from remote sensing and archive field data relevant for modeling wetland distribution? (ii) Can AI be used to map wetlands with acceptable accuracy? and (iii) What are the benefits of the resulting maps compared to existing wetland maps?
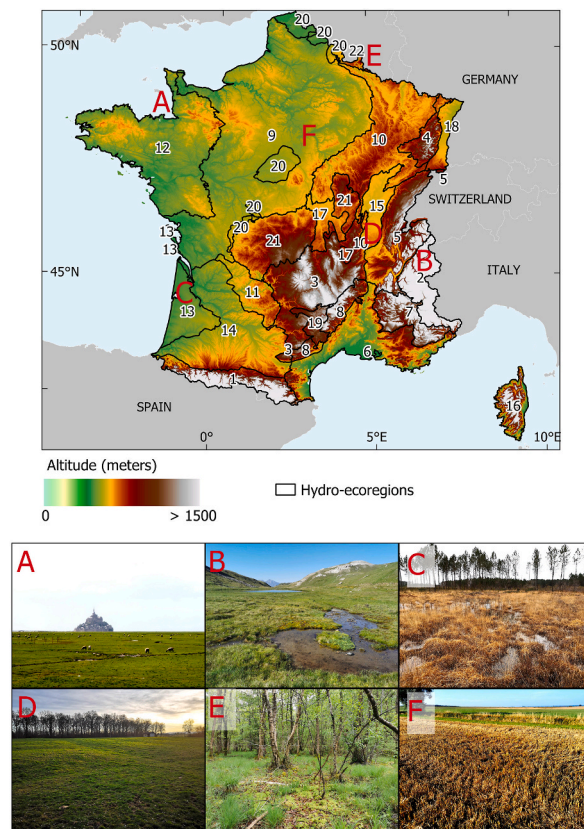
Fig. 1. Top: The study site (mainland France) divided into 22 hydro-ecoregions [64]. Bottom: Photographs of hydrogeomorphic wetland types [63] that are regularly flooded (A – estuarine-fringe, B – slope, C – depressional) or non-flooded (D – flat, E – riverine, with a forest, F – riverine, with crops).

2. Materials and methods

2.1. Study site

The study site encompasses mainland France (Fig. 1), which has high climatic, geological, and topographical variability in 22 hydro-ecoregions (HER) [64]. All hydrogeomorphic (HGM) wetland types [63] occur throughout France (Fig. 1A–F). In the 1990s, the first national map of wetlands focused on Ramsar sites and natural areas of ecological interest, which resulted in the identification of 6415 km^2 of wetlands [12]. An increasing number of local wetland mapping have been conducted since the 2000s, but their quality varies, and they cover only half of the area of France [65]. The first comprehensive national wetland map was conducted in 2014 by modeling topographical variables at 50 m spatial resolution, which estimated that wetlands covered 23% of mainland France [43]. In parallel, field-based monitoring highlighted that 41% of remarkable wetland sites experienced a decrease in conservation status [66].

2.2. Wetland mapping framework

Following the recommendations of Ling et al. [13], the national wetland mapping approach developed in this study was steered by a committee of scientists in geography, soil science, and ecology, as well as policy makers. The term "wetland" used in this study is based on the Ramsar definition: *areas of marsh, fen, peatland or water, whether natural or artificial, permanent or temporary, with water that is static or flowing, fresh, brackish or salt, including areas of marine water the depth of which at low tide does not exceed 6 m* [62]. Conceptually, this study was based on the "Potential, Existing, Efficient Wetlands" approach [38] and focused on potential wetlands, which correspond to the maximum extent of wetlands before human alterations. In other words, potential wetland mapping outlines areas where water-related ecosystems are most likely to occur [27]. This study considered all HGM wetland types [63]: riverine, depressional, slope, flat, estuarine-fringe, and lacustrine-fringe. Wetlands were mapped by modeling groundwater using environmental variables. Map accuracy was assessed using field plots that describe soil or flora. The spatial resolution of the map was 5 × 5 m, and the minimum mapping unit was 250 m^2.

2.3. Field data collection

2.3.1. Archive databases

The archive plots, which were collected by scientists, environmental organizations, and citizens over the past 30 years, were obtained from three national databases: (i) DoneSol, which contains data from soil plots, mainly in agricultural areas [67,68]; (ii) that of the NFI, which contains data from plots that describe soil and flora in wooded areas [69], and (iii) that of the National Inventory of Natural Heritage (INPN), which contains data from flora surveys, mainly in natural areas [70]. The spatial accuracy of these archive plots usually ranges from 2 to 20 m depending on the presence of tree cover, the relief, and the global positioning system (GPS) equipment used.

For the DoneSol and NFI databases, plots with the following soil types were classified as "wetland" according to the French pedological referential: Histosols, Reductisols, Redoxisols, Thalassosols, Fluviosols, or Humic Podzosols [71–73]. For the INPN database, the Ellenberg indicator for moisture [74], which consists of 12 ordinal values that range from 1 (extreme dryness) to 12 (aquatic), was used to classify plots as "wetland". It was calculated as the arithmetic mean of the Ellenberg indicators of the species in each plot. To this end, baseFlor [75], which adjusts the Ellenberg indicator for French flora, was used. Plots with mean Ellenberg indices greater than 6 or less than 3 were classified as "wetland" and "non-wetland", respectively [76]. In contrast, plots with mean Ellenberg indices of 3–6 were excluded from the analysis because it was not clear that they were wetlands, due to human disturbance that may have influenced them. In mountainous areas (>1500 m asl), plots with Ellenberg indices less than 5 (instead of 3) were classified as "non-wetland" because these areas have less human disturbance than lowland areas and specific bioclimatic conditions.

Expert-based visual inspection of well-known sites using GIS indicated that several archive plots had been misclassified. Thus, we performed a cleaning step for the collected databases. For the soil plots, we crosschecked the soil type and the depth of hydromorphic features, the latter of which was detailed in the DoneSol and NFI databases at 10 cm and 40 cm intervals, respectively. For plots in the DoneSol database, the inconsistencies were due to misclassified soil types. To correct this issue, plots classified as "wetland" and "non-wetland" without and with hydromorphic features at depths of 0–40 and 40–80 cm, respectively, were identified as outliers (except for Fluviosols and Humic Podzosols) and excluded from the analysis. Plots with missing values for the depth of hydromorphic features were also excluded. In addition, since the spatial density of "non-wetland" plots was heterogeneous, we randomly subsampled the "non-wetland" plots to obtain a maximum of five plots per 5 × 5 km grid cell. For plots in the NFI database, no obvious inconsistencies

Table 1
The number of plots originally stored and retained for analysis, and the percentage of plots assigned to the "wetland" class, by archive database (DoneSol, National Forest Invetory (NFI), and National Inventory of Natural Heritage (INPN)).

Database	No. of plots originally stored	No. of plots retained (percentage of original plots)	Percentage of retained plots classified as "wetland"
DoneSol	177,578	36,477 (21%)	52%
NFI	93,043	89,364 (96%)	28%
INPN	366,268	9967 (3%)	85%
All	**636,889**	**135,508 (21%)**	**39%**

were identified; however, its plots with Redoxisols and hydromorphic features at depths greater than 50 cm were excluded from the analysis, since some uncertainty existed about whether or not they should be classified as "wetland". The INPN database was cleaned in two steps. First, since its floristic plots had not always been collected using a phytosociological approach and it contained no information about the areas surveyed, plots with less than three species (likely threatened or invasive species) or more than 20 species (likely floristic inventories conducted over several hundred m^2) were excluded from the analysis. Second, all plots that were located in urban areas according to the national land cover map (10 m spatial resolution) [77] were excluded. While some plots had truly been surveyed in urban areas, other plots - likely surveyed without GPS - had been georeferenced to the nearest town center.

A second expert-based visual inspection of the "cleaned" plots using GIS did not reveal any particular inconsistencies. After these cleanup steps, 135,508 plots were retained from archive databases for further analysis (Table 1), with a mean density of 0.25 plots/km^2 (Fig. 2A–D).

2.3.2. Experimentally designed sampling

In the beginning of 2021, a field campaign was conducted specifically for this study using stratified sampling on either side of suspected wetland boundaries. These boundaries were identified using geological and topographical maps, aerial photography, and, when available, local wetland inventories. A total of 440 sites were surveyed throughout France, covering all HGM types [63]. At each site, the HGM type was determined, and three transects were established, with at least one plot located in a wetland and another in a non-wetland area. In each plot, a soil auger was used to measure the depth of hydromorphic features and the thickness of redoxic, reductive, or histic horizons. Vegetation type was characterized according to the European Nature Information System [78]. Each plot was georeferenced using GPS, with a mean accuracy of 3 m.

Plots that had hydromorphic features at depths less than 50 cm or typical wetland vegetation were classified as "wetland". Plots with Fluvisol and humic Podzosol soils were classified as "wetland". Plots that had hydromorphic features at depths greater than 50 cm were excluded from the analysis due to uncertainty about how to classify them. A total of 3012 plots (of which 64% were classified as "wetland") were retained for the analysis. See Gayet et al. [79] for a detailed overview of the sampling protocol and the raw field data.

2.4. Environmental variables

Topographic and geological variables were used to model the spatial distribution of wetlands (Table 2). The topographic variables were derived from the national airborne DTM at 5 m spatial resolution, which is available in open-access from the website of the French National Geographic Institute (IGN) (https://geoservices.ign.fr/). The vertical accuracy of DTMs usually ranges from 30 to 70
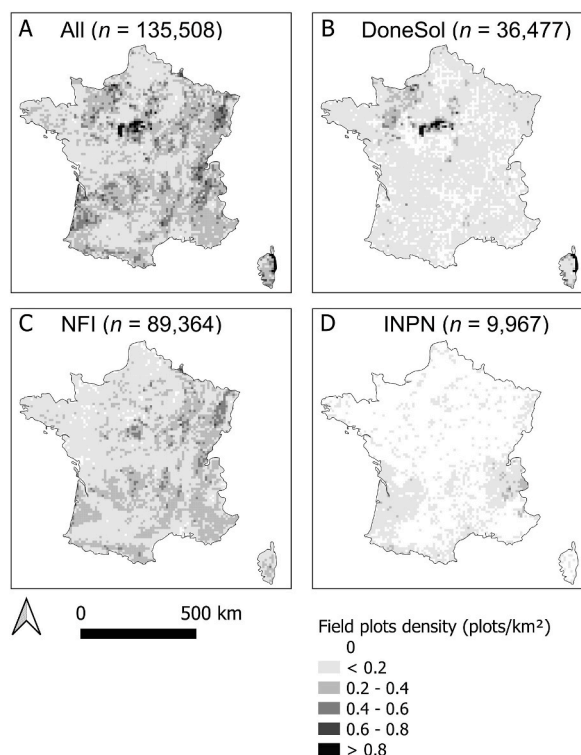

Fig. 2. Spatial distribution of field plots from the French archive databases used to calibrate or validate the random forest model: A – all databases, B – the national database of soil-survey data (DoneSol), C – the National Forest Inventory (NFI), and D – the National Inventory of Natural Heritage (INPN).

Table 2
Properties of the environmental variables used to map wetlands.

Type	Source data	Resolution/scale	Name	Acronym	Target wetlands
Geological	National Geological Map (BRGM, 2022)	1:50,000	Geological variable	GEOL	Flat and slope
Topographical	National airborne DTM (IGN, 2021)	5 m	Digital Terrain Model	DTM	Estuarine-fringe
			Topographic wetness index	TWI	Riverine
			Vertical distance to channel network	VDCN	Riverine and lacustrine-fringe
			Multi-scale topographic position index	TPI_micro TPI_meso TPI_macro	Depressional and lacustrine-fringe

cm, depending on the type of land use and the acquisition technology (e.g. LiDAR, photogrammetry) [80]. DTMs have been used as an explanatory variable to identify estuarine-fringe wetlands [81,82]. Three topographic variables were derived from this DTM: (i) the topographic wetness index (TWI), (ii) the vertical distance to the channel network (VDCN), and (iii) the multiscale topographic position index (TPI). TWI, which characterizes potential soil wetness as a function of the contributing area and local slope [83], ranges from 0 to 30, with a higher value indicating a higher probability of wet soil. TWI is appropriate for characterizing riverine wetlands in particular [60]. To remove human-built features (e.g. roads, ditches) that could influence estimated flow, the DTM was first smoothed using a median filter (7×7 window). TWI was calculated using a multi-directional flow accumulation algorithm [84], which is appropriate for characterizing biotopes [85]. VDCN expresses the vertical height (in m) between the elevation of a pixel and the nearest channel. The GIS layer of the channel network in the national hydrological database [86] was used to calculate it. VDCN is relevant for characterizing riverine and lacustrine-fringe wetlands [87]. TPI describes the position of a pixel relative to its neighborhood at a given spatial scale [88]. It represents three layers – TPI_micro, TPI_meso, and TPI_macro – that describe the position of each pixel at a micro- (5–300 m), meso- (300-1000 m), and macro- (>1000 m) scale, respectively. The distance interval for each scale was set using the Relative Topographic Position Scale Signature tool [88] at multiple sites covered by wet depressions ranging from a few m² to several thousand m². TPI were standardized to range from -2 to $+2$, with negative values indicating positions lower than the neighborhood and positive values indicating positions higher than the neighborhood. TPI is especially valuable for detecting depressional wetlands unconnected to the riverine network [50].
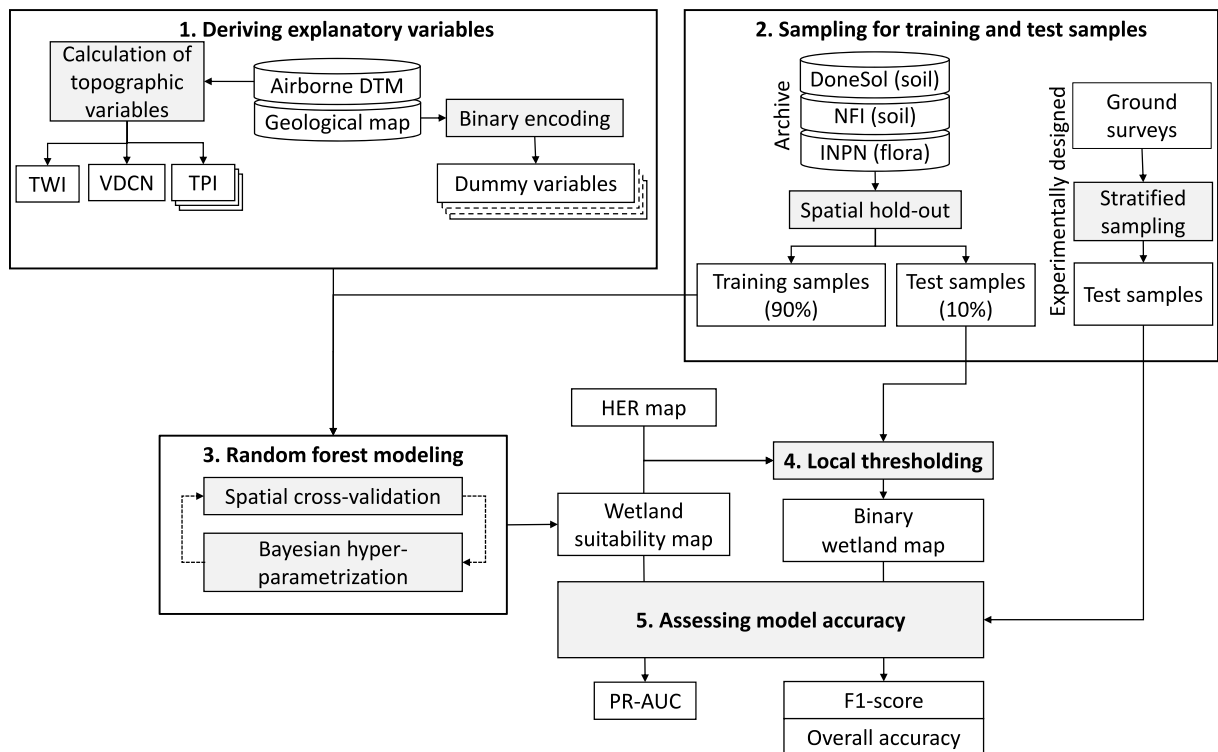
Fig. 3. Flowchart of the method used to map wetlands by modeling topographic and geological variables subsequently calibrated and validated using soil and flora field samples.

The geological variable was derived from the 1:50,000 geological map of France in vector format (BD Charm-50) and available in open-access from the website of the Bureau de Recherches Géologiques et Minières [89]. The geological variable was considered useful for detecting flat or slope wetlands that cannot be detected from topographic variables. In these areas, some parent materials (e.g., some sandstones, shales, loess, granites …) are likely to slow subsurface flow with soil saturation resulting in hydromorphic soils. Since the geological map of France contains 16,864 types of units, including this categorical variable directly into a model would have created the same number of binary variables, which would have been unworkable. To address this issue, we applied binary encoding [90], which reduced the number of binary variables to only 15. These 15 dummy variables were then rasterized at a spatial resolution of 5 m.

2.5. Artificial intelligence modeling

The AI modeling used to map wetlands consisted of five steps (Fig. 3). In a first step, explanatory variables were derived from an airborne DTM and a geological map. In a second step, training and test samples were respectively extracted from archive field databases and experimentally designed ground surveys. In a third step, a random forest modeling of wetlands was applied using explanatory variables and training samples. In a fourth step, a local thresholding was carried out on the suitability wetland map to achieve a binary map. In a fifth step, the accuracy of the suitability and binary wetland maps was assessed from independent experimentally designed test samples. Each of these 5 steps is further developed in the following sub-sections.

2.5.1. Setting explanatory variables
The dataset of exploratory variables included 21 environmental variables divided into 6 topographic variables and 1 geological variable encoded in 15 dummy variables (Table 2). The geological variables were aligned to the topographic variable grid in the French projection system (EPSG 2154) using nearest-neighbor interpolation. The size of this dataset was ca. 1 TB.

2.5.2. Training and test sampling
The field plots in the three archive databases were divided into two datasets using spatial hold-out with 10 × 10 km blocks [91]: 90% of the plots (i.e. 125,573 plots, of which 39% were wetland) were used as training samples, and the remaining 10% (11,935 plots, of which 33% were wetland) were used as first test datasets. This 10 km distance was calculated using the spatial autocorrelation distance of each explanatory variable. The field plots from the experimentally designed stratified sampling (i.e., 3012 plots, of which 64% were wetland) were used as an independent test dataset.

2.5.3. Random forest modeling
Wetland distribution was modeled for the entire study site using a single RF model [92] that has been widely used to map this ecosystem [26]. RF models have mapped wetlands more accurately than other types of models, such as support vector machine, maximum likelihood, or decision tree [14,26], since they can consider many variables from different sources and have little sensitivity to outliers and over-learning [93]. The model was calibrated using 10-fold cross-validation with a 10 × 10 km spatial constraint [91]. It was then hyper-parameterized using the Bayesian PR-AUC index, which is an appropriate performance index for binary modeling with unbalanced sampling [94]. Specifically, the parameter for the number of variables considered in each branch of the decision tree was estimated. The calibrated model was then applied to mainland France, which yielded a wetland suitability map with continuous values from 0 (low suitability) to 100 (high suitability). The importance score of each explanatory variable in the RF model was calculated as the mean decrease in accuracy divided by its standard deviation across the 10 folds, and then scaled from 0 to 100 [95]. For consistency, the importance scores of the 15 dummy geological variables were summed.

Table 3
Characteristics of the nine existing wetland maps compared to the study's binary map.

Coverage	Acronym	Description	Resolution (m)	Ground-water modeling	Open-water observations	Vegetation observations	Reference
World	CW_TCI	Composite global wetland map (topography-climate wetness index)	500	✓	✓		[35]
World	CW_WTD	Composite global wetland map (water table depth)	500	✓	✓		[35]
World	GLS	Copernicus Global Land Service (class "herbaceous wetland")	100		✓	✓	[115]
Europe	SWEDI	Spatial wetland distribution	1000	✓		✓	[42]
Europe	CLC	Copernicus CORINE Land Cover (classes "Rice fields", "Inland marshes", "Peat bogs", "Salt marshes", "Salines", "Intertidal flats", "Coastal lagoons", and "Estuaries")	100		✓	✓	[113]
Europe	RIP	Copernicus Riparian zones	25	✓	✓		[46]
Europe	WW	Copernicus Water & Wetness	10		✓		[125]
Europe	ELC10	Land cover map of Europe (class "Wetland")	10		✓	✓	[114]
France	PW	Potential wetlands	50	✓			[43]

2.5.4. Local thresholding

Thresholding, which transforms the probabilistic output of the model (wetland suitability) into a binary map (presence/absence of a wetland), is a challenging step [56]. The probabilistic output of the model was thresholded by HER to consider local environmental characteristics. Since the original HER map was produced at 1:1,000,000 scale [64], the thresholded map would have had coarse edge effects. To address this issue, HER boundaries were adjusted to those of the topographic watersheds in the national hydrological database [86]. Thresholding values were determined using the archive test dataset. Specifically, model output was thresholded by expert interpretation of changes in the OA and F1-scores as a function of the threshold value (Supplementary material S1), with OA describing the importance of the "wetland" and "non-wetland" classes, and the F1-score describing that of the "wetland" class. The range of maximum accuracy values for both OA and F1-scores was determined before selecting the threshold that yielded the highest accuracy within these ranges. Visual inspection of the resulted binary map was then performed using GIS for each HER to validate the threshold set.

2.5.5. Accuracy assessment

The second test dataset (i.e., derived from the experimentally designed sampling) was used to assess (by HER) the overall and local accuracy of the suitability map (using the PR-AUC) and the binary map (using the F1-score and OA).

2.6. Comparison to existing wetland maps

The accuracy of the binary map was compared to those of nine existing wetland maps with a global, European, or national coverage (Table 3). Local wetland field inventories were not considered since they covered only ca. half of mainland France in 2022. Soil plots that had hydromorphic features at depths of 30–50 cm were excluded from test datasets for the comparative analysis, since their classification as "wetland" may have depended on the definition used to build each of the nine wetland maps. As a result, 2603 experimentally designed test plots (of which 58% were wetland) were used in the comparative analysis. A more detailed comparison to the nine wetland maps was also performed by HGM type.

All analyses were performed using R software version 3.6.0 (R Core Team, 2019) and its blockCV [91], caret [96], terra [97], RSAGA [98], whitebox [99], and rgdal [100] packages. The maps were visually inspected and GIS figures were generated using QGIS software version 2.18.22 [101].
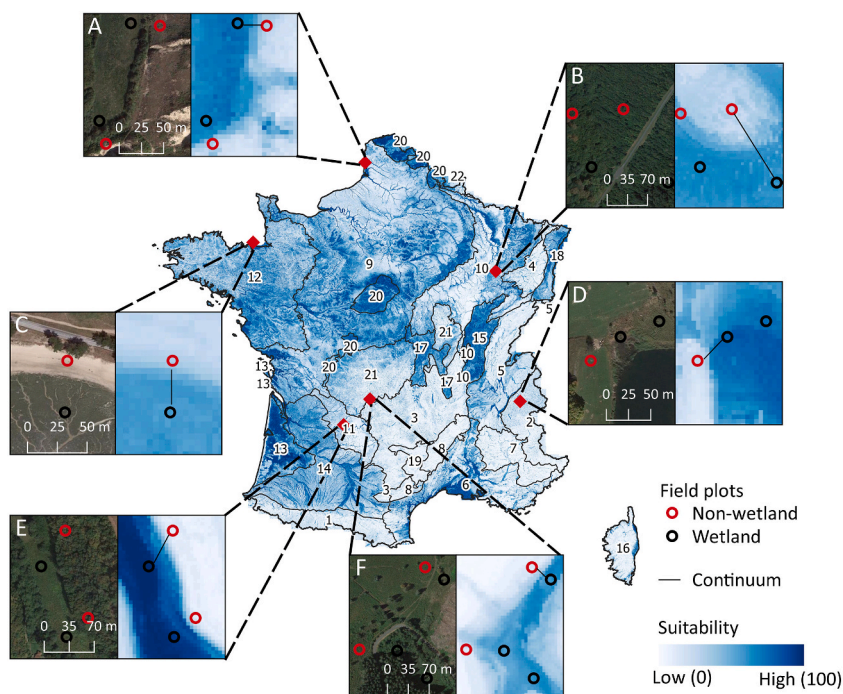
Fig. 4. Map of wetland suitability in mainland France derived from random forest modeling of topographic and geological variables. Each insert map focuses on a specific type of hydrogeomorphic wetland: A – depressional, B – flat, C – estuarine-fringe, D – lacustrine-fringe, E – riverine, and F – slope.

3. Results

3.1. Wetland map

In the RF model's wetland suitability map, major valleys such as the Saône plain (HER 15) and the Rhine plain (HER 18) were evident, as were the Camargue (HER 6), the Gascogne moors (HER 13), and the Scarpe-Escault and Sologne sandy-clay marshes (HER 20) (Fig. 4). In more detailed maps, the fine-grained pattern of the predicted suitability of each HGM type was clearly visible (Fig. 4 A–F). In addition, the suitability predicted by the RF model was consistent with the field transects located on the wetland-*continuum*.

When comparing this study's binary map to the nine existing wetland maps for a Ramsar peatland (Fig. 5 A–K), the former was the most consistent with the field plots (Fig. 5 B). The advantage of using high spatial resolution (5 m) to define the fine-grained pattern of wetlands was clear when compared to the PW (50 m) or Composite global wetland (500 m) maps (Fig. 5 C, E, F). The Copernicus Water & Wetness map of Europe and Land cover map of Europe also have a fine-grained pattern (10 m), but they had high under- and/or over-detection bias (Fig. 5 H, K). In the other maps, large (Spatial wetland distribution (SWEDI), Copernicus CORINE Land Cover) or very large (Copernicus Riparian zones, Copernicus Global Land Service) under-detection bias was also observed (Fig. 5 D, G, I, J).

3.2. Model accuracy

For mainland France, the RF model's suitability output had high statistical accuracy (test PR-AUC 0.76). Similar PR-AUC values for training (0.84, SD 0.01) highlighted little over-learning of the RF model. The RF model's binary output also had satisfactory accuracy (F1-score 0.75, OA 0.67).

The importance of explanatory variables to the model's accuracy varied: VDCN, and to a lesser extent TWI and DTM, were the most important variables, while the geological and TPI variables had lower but nonetheless high importance (Fig. 6).

At the local scale (HERs), the optimal thresholding value varied greatly, ranging from 0.15 for HER 2 to 0.62 for HER 18 (Supplementary material S1). Model accuracy also varied per HER (Table 4). Specifically, the accuracy of the wetland suitability map ranged from lower values (PR-AUC 0.69 and 0.68) for HER 11 and 16 to higher values (PR-AUC 0.98 and 0.90) for HER 15 and 20. The accuracy of the binary map ranged from lower values for HER 21 (F1-score 0.43 and OA 0.53) and HER 6 (F1-score 0.63 and OA 0.51)
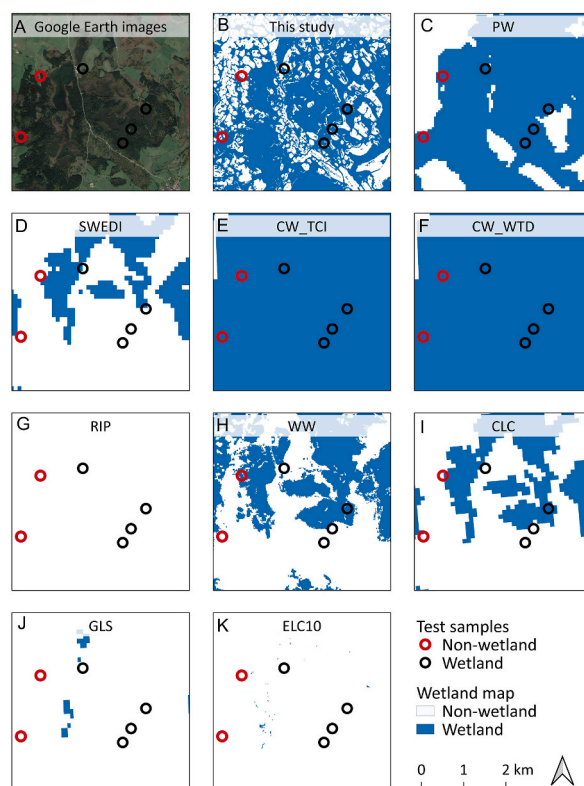
Fig. 5. Comparison of the binary wetland map modeled in this study to the nine existing wetland maps of Ramsar peatland site 1266 in France ("Tourbières et lacs de la Montagne jurassienne", 46.82°N, 6.13°E): A – Google Earth Images, B – This study, C – PW (Potential wetlands), D – SWEDI (Spatial wetland distribution), E – CW_TCI (Composite global wetland map - topography-climate wetness index), F – CW_WTD (Composite global wetland map - water table depth), G – RIP (Copernicus Riparian zones), H – WW (Copernicus Water & Wetness), I – CLC (Copernicus CORINE Land Cover), J – GLS (Copernicus Global Land Service), K – ELC10 (Land cover map of Europe). The characteristics of the maps are described in Table 3.
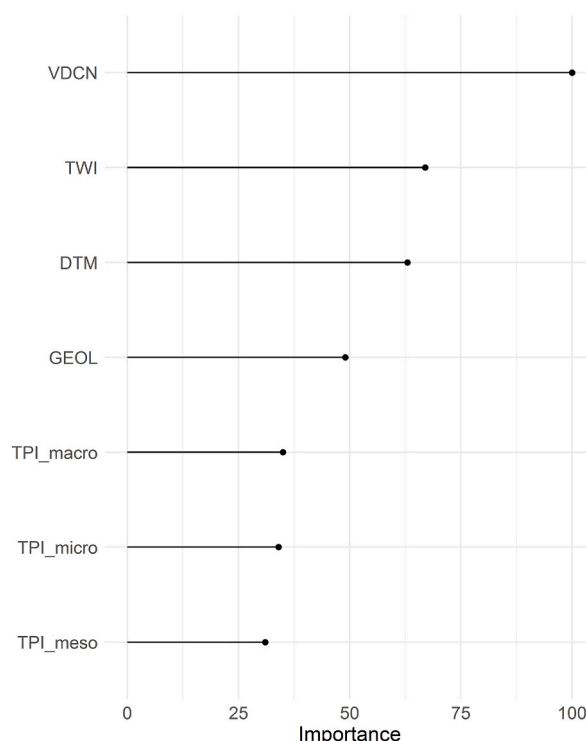
Fig. 6. Importance of the explanatory variables used by the random forest model to map wetlands. See Table 2 for definitions of the variable abbreviations.

Table 4

Accuracy by hydro-ecological region (HER) of wetland suitability maps (based on the precision-recall area under the curve (PR-AUC)) and binary maps (based on the F1-score and overall accuracy (OA)) calculated from the experimentally designed test dataset. na: not applicable.

HER	Samples	PR-AUC	F1-score	OA
1	0	na	na	na
2	203	0.70	0.72	0.59
3	335	0.81	0.74	0.73
4	0	na	na	na
5	173	0.72	0.77	0.72
6	92	0.71	0.63	0.51
7	0	na	na	na
8	39	0.92	0.84	0.79
9	341	0.74	0.71	0.60
10	375	0.74	0.74	0.63
11	110	0.69	0.68	0.61
12	765	0.85	0.79	0.70
13	130	0.81	0.81	0.72
14	78	0.69	0.78	0.67
15	103	0.98	0.99	0.97
16	72	0.68	0.68	0.61
17	0	na	na	na
18	0	na	na	na
19	0	na	na	na
20	16	0.90	0.93	0.88
21	138	0.74	0.43	0.53
22	42	0.83	0.76	0.74

to higher values for HER 15 (F1-score 0.99 and OA 0.97) and HER 20 (F1-score 0.93 and OA 0.88). It should be noted that the suitability and binary maps had similar accuracy ranges for all HERs, except HER 21, for which the suitability map was highly accurate (PR-AUC 0.74), but the binary map was not (F1-score 0.43).

The RF model's binary map was significantly more accurate than the nine existing wetland maps (F1-score at least 0.14 points higher) (Table 5). Moreover, existing maps based on groundwater modeling (highest F1-score of 0.59 for the Potential wetlands map of France (PW)) were more accurate than those based only on open-water or vegetation observations (highest F1-score of 0.12 for the

Table 5
Accuracy of the binary wetland map modeled in this study and of the nine existing wetland maps, in descending order of the F1-score. OA = overall accuracy, UA = user's accuracy, PA = producer's accuracy. See Table 3 for definitions of the map abbreviations.

Map	F1-score	OA	UA	PA
This study	0.73	0.66	0.68	0.78
PW	0.59	0.57	0.66	0.54
CW_TCI	0.43	0.48	0.59	0.33
CW_WTD	0.40	0.47	0.58	0.30
SWEDI	0.30	0.48	0.70	0.19
RIP	0.12	0.44	0.63	0.07
WW	0.12	0.44	0.69	0.06
CLC	0.04	0.43	0.69	0.02
GLS	0.01	0.42	0.58	0.01
ELC10	0.01	0.42	1.00	0.00

Copernicus Water & Wetness map of Europe). Furthermore, the model used to produce the binary map provided the best trade-off between user accuracy (0.68) and producer accuracy (0.78) compared to existing maps, such as SWEDI or ELC10, which provide higher user accuracy (respectively 0.70 and 1.00) but much lower producer accuracy (respectively 0.19 and 0.00).

The RF model's binary map was more accurate than any of the nine existing maps, regardless of HGM type (Table 6). Specifically, the largest increases in accuracy of this study's map were for flat (+0.28 in F1-score and +0.24 in OA) and slope wetlands (+0.17 in F1-score and +0.06 in OA), followed by riverine and depressional wetlands (+0.12 in F1-score and +0.08 in OA for both HGM). In contrast, the RF model used in this study only slightly improved the mapping accuracy of lacustrine fringes (+0.04 in F1-score and +0.02 in OA) and estuarine fringes (+0.03 in F1-score and +0.01 in OA). Even with the increased accuracy, the depressional and slope wetlands were still identified least well (F1-scores 0.69–0.70, OA 0.63–0.66).

4. Discussion

4.1. Are environmental variables derived from remote sensing and archive field data relevant for modeling wetland distribution?

In this study, mining archive databases provided free and ready access to several hundred thousand real field samples distributed evenly over mainland France, which is many more than the 16,000 or 24,000 samples used for the national wetland mapping in China [31] and Canada [33], respectively. In the absence of archive databases, collecting so many real field samples would have been impossible given budget and time constraints [14].

Although well structured, field archive databases inevitably contain "hidden" errors [102], especially related to geolocation and interpretation of the plots [52,103]. For example, the geolocation accuracy of some plots is likely to be approximate, especially for older plots collected with older GPS devices (±20 m). However, uncertainty probably influences model results little, since archive plots were rarely located near wetland boundaries. To decrease uncertainty in the interpretation of plots as much as possible, we verified the consistency between soil type and the depth of hydromorphic features. Despite this cleaning step, the samples probably still contained outliers. Nonetheless, several studies indicate that outliers have relatively little influence on the accuracy of RF models [93,104].

The topographic variables in this study had a spatial resolution of 5 m, which is unprecedented at the national scale, at which coarser-resolution (30–50 m) variables are usually used [27,31,43,44]. This was possible only by using the open-access DTM of IGN. Despite the known value of DTMs for mapping wetlands [16,17,42], we initially did not plan to include geological or soil variables in the model due to their qualitative format. However, preliminary tests based on topographic variables alone revealed that wetlands were under-detected on clay or marl flats. Since soil maps were not available at a fine spatial scale, we used the geological map. The

Table 6
Accuracy (F1 = F1-score, OA = overall accuracy) of the binary wetland map modeled in this study and of the nine existing wetland maps by hydrogeomorphic (HGM) type, in descending order of the F1-score. See Table 3 for definitions of the map abbreviations. *n* refers to the number of test samples used to calculate the accuracy indices per HGM type.

Map	Riverine (n = 953) F1	OA	Depressional (n = 228) F1	OA	Slope (n = 695) F1	OA	Soil flats (n = 501) F1	OA	Estuarine fringes (n = 97) F1	OA	Lacustrine fringes (n = 129) F1	OA
This study	0.76	0.68	0.70	0.66	0.69	0.63	0.80	0.72	0.75	0.67	0.75	0.70
PW	0.64	0.60	0.58	0.58	0.52	0.57	0.52	0.48	0.72	0.66	0.71	0.68
CW_TCI	0.49	0.51	0.53	0.47	0.25	0.47	0.38	0.43	0.69	0.55	0.48	0.50
CW_WTD	0.48	0.51	0.49	0.45	0.19	0.46	0.31	0.39	0.68	0.56	0.48	0.49
SWEDI	0.29	0.49	0.44	0.56	0.12	0.46	0.39	0.46	0.41	0.43	0.33	0.50
RIP	0.25	0.47	0.05	0.47	0.03	0.45	0.01	0.32	0.15	0.47	0.10	0.45
WW	0.07	0.44	0.20	0.51	0.10	0.47	0.04	0.33	0.48	0.58	0.21	0.47
CLC	0.02	0.44	0.09	0.48	0.04	0.45	0.00	0.31	0.26	0.48	0.18	0.50
GLS	0.01	0.43	0.05	0.48	0.00	0.45	0.00	0.32	0.00	0.43	0.08	0.44
ELC 10	0.00	0.43	0.03	0.48	0.00	0.45	0.00	0.32	0.00	0.43	0.05	0.46

automatic binary encoding of this qualitative variable into a quantitative format avoided a subjective and time-consuming expert--based transformation. This geological variable, which had relatively high importance for model accuracy, effectively corrected the biases observed for flat wetlands.

VDCN was clearly the most important variable for mapping the wetlands of mainland France, perhaps due to the dominance of riparian wetlands, for which VDCN is important [41,43,46]. The quality of VDCN depends on the completeness of the vector layer of the hydrographic network. Although this layer is of relatively good quality in France and has been validated through many field campaigns, it remains non-exhaustive, especially near springs. Visual inspections revealed that TWI supplemented VDCN well. TWI was the second-most important variable in the model, which supports studies of Higginbottom et al. [48] and Chignell et al. [60], who recommended generating TWI at a very high spatial resolution to map wetlands. A DTM, which contained the raw data used to generate the other topographic variables, was considered an explanatory variable to identify estuarine-fringe wetlands [81]. Although these types of wetlands cover a large area on the French coastline, the high importance of the DTM for the model was unexpected. In contrast, although the TPI variables successfully identified some unconnected depressions (Table 6, Fig. 4A), we expected them to have more importance. They may have had lower importance due to over-detection, since the model predicted that all depressions were wetlands [28], which is not always true.

The results of using four topographic variables and one geological variable to better map all HGM types in mainland France are encouraging, even though slope and depressional wetlands were mapped the least accurately. Using satellite-derived variables to characterize soil moisture via SAR [29] and/or thermal sensors [105,106] could increase the accuracy of mapping these HGM types.

4.2. Can AI be used to map wetlands with acceptable accuracy?

In this study, a single RF model was used to produce a national wetland map with good accuracy and low over-fitting, despite the high biogeographic diversity throughout mainland France. This study addressed this methodological issue using an independent metric of threshold accuracy (i.e., PR-AUC), which was well suited to the model's raw probabilistic output. In addition, we used spatial blocks of 10×10 km during cross-validation to avoid the influence of spatial autocorrelation.

In agreement with Chignell et al. [60], we considered the wetland suitability map as the most informative output. However, we also derived a binary map to compare it to existing wetland maps and meet requests of french wetland managers and policy makers. The thresholding step, which converts a suitability map into a binary map, is often considered challenging in wetland inventories [31,44, 45]. In this study, we used accuracy indices (F1-score and OA) to apply a locally specific and expert-based threshold. Our results highlight that the commonly applied default threshold of 0.5 [46] is likely not optimal, with lower thresholds for mountainous areas (e. g. HER 1 and 2) and higher thresholds for lowland areas (e.g. HER 12 and 18). This supports the research of Mao et al. [31], who adjusted thresholds by ecological region to map wetlands in China.

The expert-based threshold in this study was determined from real field samples, which provides good reliability, but requires more samples than those used to fit the model. Feasible alternatives when there are too few field samples include collecting pseudo field samples by visually interpreting images at very high spatial resolution [44] or using Ostu's thresholding method [45]. As Rebelo et al. [24] indicated, the expert and local thresholding approach requires map users to adjust the threshold based on their own expertise. For example, user participation would be desirable for HER 21, in which the small number of samples probably resulted in a non-optimal threshold given the large range of accuracy of the suitability and binary maps.

The OA of this study's wetland map (67%) is lower than that of other studies, such as 82% in Albania [45], 86% in Canada [33], and 95% in China [31]. This could be due to the validation method used, since accuracy in the other studies was calculated from samples collected mainly by visually interpreting remote sensing images at very high spatial resolution, and not from real fields, which were sometimes collected far from wetland boundaries, which increases uncertainty when assessing the accuracy of wetland maps [16]. In contrast, the validation protocol applied in this study followed best practice recommendations by using real independent field plots [107] collected along wetland/non-wetland transects [108], which yielded a lower but more reliable estimate of model accuracy [54].

Model accuracy differed among regions, perhaps due to the distribution of "wet soil" archive samples in the landscape: accuracy was lowest for regions with major limestone uplands (HER 11) and for Corsica (HER 16), where wetlands are rare and the probability of having a "wet soil" archive sample is low. In contrast, accuracy was highest for regions covered by a large proportion of wetlands, such as the Saône plain (HER 15) or regions with sandy-clay deposits (HER 20), where a "wet soil" archive sample is more likely.

The costs of this study were low. The archive data, DTM, geological map, and software used were free, and data were processed on a university server (Intel® Xeon® 2.1 GHz, 48 cores, 384 GB RAM). The highest costs were for human resources, which included employing (i) one geomatics engineer for one year to collect and harmonize the archive data, generate the explanatory variables, and develop the script, and (ii) three ecological engineers for nine months each to collect validation plots. From an operational viewpoint, it took much less time to run the model (ca. 5 days for mainland France) than to prepare the data (especially to harmonize the archive databases) and design the script.

Given the large number of samples available, future analysis will focus on applying deep-learning modeling, which several studies have described as useful for characterizing wetlands [109–111]. In addition, mapping HGM types within a wetland mask [112] would be an interesting approach for assessing wetland functions.

4.3. What are the benefits of the resulting maps compared to existing wetland maps?

Two main insights emerged from comparing the study's maps to existing wetland maps. First, our model generated a wetland suitability map, which had been previously provided only by the Copernicus Riparian zones map [46]. Second, the study's binary map

is more accurate than the wetland maps produced in other previous studies for the following reasons: (i) we used environmental variables that consider both existing and damaged wetlands rather than vegetation, soil and water indices that consider only existing wetlands [113–115]; (ii) we used a high spatial resolution DTM (5 m), which allowed small wetlands (depressions, springs) to be better identified and refined the delineation of large wetlands [41], compared to broader spatial resolution DTMs [35,42]; and (iii) we combined complementary environmental variables, especially the multiscale TPI and a geological variable, which better identified all HGM types, notably flat and depressional ones that were often omitted [43,46]. The SWEDI and the Composite global wetland maps may have had lower accuracy in part due to the mismatch between their resolution (≥500 m) and the fine scale of the experimentally designed samples used to validate them.

Since wetlands are fine-grained and scattered distributed ecosystems, our fine-scale maps will help to better target conservation policies at different scales. At the global scale, these maps will improve the implementation of the Ramsar Strategic Plan 2016–2024 (targets 5 'maintenance of ecological character' and 12 'restoration') [116], the Aichi Biodiversity (Targets 1 'conserve biodiversity', 5 'Habitat loss halved or reduced' and 11 'conserve at least 17% of terrestrial and inland water, and 10% of coastal and marine areas') [117], the UN Sustainable Development Goals (targets 6.6 'protect and restore water-related ecosystems' and 15.1 'ensure the conservation … of terrestrial and inland freshwater ecosystems') [118], but also the Paris Agreement on Climate Change [119]. At the European scale, these maps will refine the areas within which the status of wetlands is assessed for the Water Framework Directive [120] and the Habitat Directive [121] reporting. At the national scale, these maps will contribute to the mapping of green corridors [122], will support biodiversity plans [123] and the assessment of ecosystems and ecosystem services [124]. At the local scale, these maps can help refine wetland inventories and urban plans, for example to prevent scattered urbanization, or to restore damaged wetland areas. These maps can also be used as a communication tool to raise awareness among citizens and decision-makers on wetland conservation.

Wetland mapping is an ongoing process that is updated as technological advances and new data become available [13]. Considering existing inventories for France and based on the groundwater-modeling approach, version 1 would be the SWEDI map [42] at 1 km spatial resolution, version 2 would be the PW map at 50 m spatial resolution [43], and version 3 would be this study's map at 5 m spatial resolution.

5. Conclusion

This study highlighted that a national wetland mapping with a fine-grained pattern (5 m) and a good accuracy can be produced automatically by AI using archive field data and free environmental variables. The results showed that: (i) all wetlands were identified regardless of their HGM type (riverine, depressional, slope, soil flats, estuarine fringes, and lacustrine fringes) or status (existing or damaged); (ii) the suitability map revealed the wetland-non-wetland *continuum*; (iii) the binary map was more accurate than existing wetland maps; (iv) the high spatial resolution (5 m) of the wetland maps enabled more targeted conservation measures; and (v) the operational and low-cost approach developed to map wetlands in mainland France can be transferred to other countries. This study also highlighted two methodological limitations: (i) the proposed approach is based on the definition of a threshold value to produce the binary wetland map, which was challenging but could be refined based on local field expertise, and (ii) the accuracy of slope and depression wetland modeling was moderate and needed improvements. Using satellite variables that combine soil moisture and new deep-learning models is a promising avenue to further improve identification of these threatened ecosystems.

Author contribution statement

SEBASTIEN RAPINEL; Laurence Hubert-Moy: Conceived and designed the experiments; Analyzed and interpreted the data; Wrote the paper.

Léa Panhelleux: Performed the experiments.

Guillaume Gayet; Blandine Lemercier; Bertrand Laroche: Analyzed and interpreted the data; Contributed reagents, materials, analysis tools or data.

François Chambaud; Anis Guelmami; Rachel Vanacker: Analyzed and interpreted the data.

Data availability statement

Data will be made available on request.

Declaration of interest's statement

The authors declare no conflict of interest.

Acknowledgements

Appendix A. Supplementary data

Supplementary data to this article can be found online at https://doi.org/10.1016/j.heliyon.2023.e13482.

References

[1] X. Xu, M. Chen, G. Yang, B. Jiang, J. Zhang, Wetland ecosystem services research: a critical review, Glob. Ecol. Conser. 22 (2020), e01027, https://doi.org/10.1016/j.gecco.2020.e01027.

[2] W.V. Reid, H.A. Mooney, A. Cropper, D. Capistrano, S.R. Carpenter, K. Chopra, P. Dasgupta, T. Dietz, A.K. Duraiappah, R. Hassan, Ecosystems and Human Well-Being-Synthesis: A Report of the Millennium Ecosystem Assessment, Island Press, 2005.

[3] S.E. Darrah, Y. Shennan-Farpón, J. Loh, N.C. Davidson, C.M. Finlayson, R.C. Gardner, M.J. Walpole, Improvements to the Wetland Extent Trends (WET) index as a tool for monitoring natural and human-made wetlands, Ecol. Indicat. 99 (2019) 294–298.

[4] N.C. Davidson, L. Dinesen, S. Fennessy, C.M. Finlayson, P. Grillas, A. Grobicki, R.J. McInnes, D.A. Stroud, Trends in the ecological character of the world's wetlands, Mar. Freshw. Res. 71 (2019) 127–138.

[5] C. Perennou, E. Gaget, T. Galewski, I. Geijzendorffer, A. Guelmami, Chapter 11 - evolution of wetlands in mediterranean region, in: M. Zribi, L. Brocca, Y. Tramblay, F. Molle (Eds.), Water Resources in the Mediterranean Region, Elsevier, 2020, pp. 297–320, https://doi.org/10.1016/B978-0-12-818086-0.00011-X.

[6] S. Hu, Z. Niu, Y. Chen, L. Li, H. Zhang, Global wetlands: potential distribution, wetland loss, and status, Sci. Total Environ. 586 (2017) 319–327, https://doi.org/10.1016/j.scitotenv.2017.02.001.

[7] H. Čížková, J. Květ, F.A. Comín, R. Laiho, J. Pokorný, D. Pithart, Actual state of European wetlands and their possible future in the context of global climate change, Aquat. Sci. 75 (2013) 3–26, https://doi.org/10.1007/s00027-011-0233-4.

[8] W.R. Moomaw, G.L. Chmura, G.T. Davies, C.M. Finlayson, B.A. Middleton, J.E. Perry, N. Roulet, A.E. Sutton-Grier, The relationship between wetlands and a changing climate, Wetlands 38 (2018) 183–205.

[9] Y. Xi, S. Peng, P. Ciais, Y. Chen, Future impacts of climate change on inland Ramsar wetlands, Nat. Clim. Change 11 (2021) 45–51.

[10] R.J. Nicholls, Coastal flooding and wetland loss in the 21st century: changes under the SRES climate and socio-economic scenarios, Global Environ. Change 14 (2004) 69–86.

[11] N.C. Davidson, C.M. Finlayson, N.C. Davidson, C.M. Finlayson, Extent, regional distribution and changes in area of different classes of wetland, Mar. Freshw. Res. 69 (2018) 1525–1533, https://doi.org/10.1071/MF17377.

[12] J.M.R. Hughes, The current status of European wetland inventories and classifications, Vegetatio 118 (1995) 17–28, https://doi.org/10.1007/BF00045187.

[13] J.E. Ling, M.G. Hughes, M. Powell, A.L. Cowood, Building a national wetland inventory: a review and roadmap to move forward, Wetl. Ecol. Manag. 26 (2018) 805–827, https://doi.org/10.1007/s11273-018-9611-1.

[14] M.W. Lang, S. Purkis, V.V. Klemas, R.W. Tiner, Promising developments and future challenges for remote sensing of wetlands, in: Remote Sensing of Wetlands: Applications and Advances, 2015.

[15] W.J. Mitsch, J.G. Gosselink, Wetlands, in: Fifth Edi-Tion, John Wiley and Sons, Inc, Hoboken, NJ, 2015.

[16] J.R. Dymond, M. Sabetizade, P.F. Newsome, G.R. Harmsworth, A.-G. Ausseil, Revised extent of wetlands in New Zealand, N. Z. J. Ecol. 45 (2021) 1–8.

[17] R. Bou Kheir, M.H. Greve, P.K. Bøcher, M.B. Greve, R. Larsen, K. McCloy, Predictive mapping of soil organic carbon in wet cultivated lands using classification-tree based models: the case study of Denmark, J. Environ. Manag. 91 (2010) 1150–1160, https://doi.org/10.1016/j.jenvman.2010.01.001.

[18] D. Arrouays, P. Lagacherie, A.E. Hartemink, Digital soil mapping across the globe, Geoderma Reg. 9 (2017) 1–4, https://doi.org/10.1016/j.geodrs.2017.03.002.

[19] G.M. Foody, Harshness in image classification accuracy assessment, Int. J. Rem. Sens. 29 (2008) 3137–3158, https://doi.org/10.1080/01431160701442120.

[20] N. Pettorelli, M. Wegmann, A. Skidmore, S. Mücher, T.P. Dawson, M. Fernandez, R. Lucas, M.E. Schaepman, T. Wang, B. O'Connor, R.H.G. Jongman, P. Kempeneers, R. Sonnenschein, A.K. Leidner, M. Böhm, K.S. He, H. Nagendra, G. Dubois, T. Fatoyinbo, M.C. Hansen, M. Paganini, H.M. de Klerk, G.P. Asner, J.T. Kerr, A.B. Estes, D.S. Schmeller, U. Heiden, D. Rocchini, H.M. Pereira, E. Turak, N. Fernandez, A. Lausch, M.A. Cho, D. Alcaraz-Segura, M.A. McGeoch, W. Turner, A. Mueller, V. St-Louis, J. Penner, P. Vihervaara, A. Belward, B. Reyers, G.N. Geller, Framing the concept of satellite remote sensing essential biodiversity variables: challenges and future directions, Rem. Sens. Ecol. Conser. 2 (2016) 122–131, https://doi.org/10.1002/rse2.15.

[21] M. Guo, J. Li, C. Sheng, J. Xu, L. Wu, A review of wetland remote sensing, Sensors 17 (2017) 777, https://doi.org/10.3390/s17040777.

[22] C. Perennou, A. Guelmami, M. Paganini, P. Philipson, B. Poulin, A. Strauch, C. Tottrup, J. Truckenbrodt, I.R. Geijzendorffer, Mapping Mediterranean wetlands with remote sensing: a good-looking map is not always a good map, in: Advances in Ecological Research, Elsevier, 2018, pp. 243–277.

[23] Z. Niu, P. Gong, 6.05 - large-scale wetland mapping and evaluation, in: S. Liang (Ed.), Comprehensive Remote Sensing, Elsevier, Oxford, 2018, pp. 45–77, https://doi.org/10.1016/B978-0-12-409548-9.10381-1.

[24] L.-M. Rebelo, C.M. Finlayson, A. Strauch, A. Rosenqvist, C. Perennou, C. Tottrup, L. Hilarides, M. Paganini, N. Wielaard, F. Siegert, The Use of Earth Observation for Wetland Inventory, Assessment and Monitoring, Ramsar Technical Report, 2018.

[25] B.O. Wilen, M.K. Bates, The US fish and wildlife service's national wetlands inventory project, in: Classification and Inventory of the World's Wetlands, Springer, 1995, pp. 153–169.

[26] S. Mahdavi, B. Salehi, J. Granger, M. Amani, B. Brisco, W. Huang, Remote sensing for wetland classification: a comprehensive review, GIScience Remote Sens. 55 (2018) 623–658.

[27] K. Weise, R. Höfer, J. Franke, A. Guelmami, W. Simonson, J. Muro, B. O'Connor, A. Strauch, J. Flink, J. Eberle, E. Mino, S. Thulin, P. Philipson, E. van Valkengoed, J. Truckenbrodt, F. Zander, A. Sánchez, C. Schröder, F. Thonfeld, E. Fitoka, E. Scott, M. Ling, M. Schwarz, I. Kunz, G. Thürmer, A. Plasmeijer, L. Hilarides, Wetland extent tools for SDG 6.6.1 reporting from the satellite-based wetland observation service (SWOS), Rem. Sens. Environ. 247 (2020), 111892, https://doi.org/10.1016/j.rse.2020.111892.

[28] M. Singh, R. Sinha, A basin-scale inventory and hydrodynamics of floodplain wetlands based on time-series of remote sensing data, Rem. Sens. Lett. 13 (2022) 1–13.

[29] S. Adeli, B. Salehi, M. Mahdianpari, L.J. Quackenbush, B. Brisco, H. Tamiminia, S. Shaw, Wetland monitoring using SAR data: a meta-analysis and comprehensive review, Rem. Sens. 12 (2020) 2190.

[30] J.R. Melton, E. Chan, K. Millard, M. Fortier, R.S. Winton, J.M. Martín-López, H. Cadillo-Quiroz, D. Kidd, L.V. Verchot, A map of global peatland extent created using machine learning (Peat-ML), Geosci. Model Dev. Discuss. (GMDD) (2022) 1–44, https://doi.org/10.5194/gmd-2021-426.

[31] D. Mao, Z. Wang, B. Du, L. Li, Y. Tian, M. Jia, Y. Zeng, K. Song, M. Jiang, Y. Wang, National wetland mapping in China: a new product resulting from object-based and hierarchical classification of Landsat 8 OLI images, ISPRS J. Photogrammetry Remote Sens. 164 (2020) 11–25, https://doi.org/10.1016/j.isprsjprs.2020.03.020.

[32] S. Panigrahy, Mapping of wetlands using satellite remote sensing data: Indian experience, in: B.A.K. Prusty, R. Chandra, P.A. Azeez (Eds.), Wetland Science : Perspectives from South Asia, Springer India, New Delhi, 2017, pp. 423–448, https://doi.org/10.1007/978-81-322-3715-0_22.

[33] M. Mahdianpari, B. Brisco, J. Granger, F. Mohammadimanesh, B. Salehi, S. Homayouni, L. Bourgeau-Chavez, The third generation of pan-canadian wetland map at 10 m resolution using multisource earth observation data on cloud computing platform, IEEE J. Sel. Top. Appl. Earth Obs. Rem. Sens. 14 (2021) 8789–8803.

[34] S. Adeli, B. Salehi, M. Mahidanpari, L.J. Quackenbush, Toward a multi-source remote sensing wetland inventory of the USA: preliminary results on wetland inventory of Minnesota, ISPRS annals of the photogrammetry, Rem. Sens. Spat. Inform. Sci. 3 (2021) 97–100.

[35] A. Tootchi, A. Jost, A. Ducharne, Multi-source global wetland maps combining surface water imagery and groundwater constraints, Earth Syst. Sci. Data 11 (2019) 189–220.

[36] H. Van Deventer, L. Van Niekerk, J. Adams, M.K. Dinala, R. Gangat, S.J. Lamberth, M. Lötter, N. Mbona, F. MacKay, J.L. Nel, National Wetland Map 5: an improved spatial extent and representation of inland aquatic and estuarine ecosystems in South Africa, WaterSA 46 (2020) 66–79.

[37] C. Perennou, C. Beltrame, A. Guelmami, P. Tomàs Vives, P. Caessteker, Existing areas and past changes of wetland extent in the Mediterranean region: an overview, Ecol. Mediterr. 38 (2012) 53–66, https://doi.org/10.3406/ecmed.2012.1316.

[38] P. Mérot, L. Hubert-Moy, C. Gascuel-Odoux, B. Clement, P. Durand, J. Baudry, C. Thenail, A method for improving the management of controversial wetland, Environ. Manag. 37 (2006) 258–270.

[39] E. Uuemaa, S. Ahi, B. Montibeller, M. Muru, A. Kmoch, Vertical accuracy of freely available global digital elevation models (ASTER, AW3D30, MERIT, TanDEM-X, SRTM, and NASADEM), Rem. Sens. 12 (2020) 3482.

[40] X. Liu, Airborne LiDAR for DEM generation: some critical issues, Prog. Phys. Geogr. 32 (2008) 31–49, https://doi.org/10.1177/0309133308089496.

[41] S. Rapinel, E. Fabre, S. Dufour, D. Arvor, C. Mony, L. Hubert-Moy, Mapping potential, existing and efficient wetlands using free remote sensing data, J. Environ. Manag. 247 (2019) 829–839, https://doi.org/10.1016/j.jenvman.2019.06.098.

[42] C. Schleupner, U.A. Schneider, GIS-based estimation of wetland conservation potentials in Europe, Appl. Ecol. Environ. Res. 10 (2012) 385–403.

[43] L. Berthier, L. Guzmova, B. Laroche, S. Lehmann, H. Squividant, M. Martin, J.-P. Chenu, E. Thiry, B. Lemercier, M. Bardy, P. Mérot, C. Walter, Spatial prediction of potential wetlands at the French national scale based on hydroecoregions stratification and inference modelling, 2014. http://adsabs.harvard.edu/abs/2014EGUGA..1612780B. (Accessed 8 January 2016). accessed.

[44] S. Steinbach, N. Cornish, J. Franke, K. Hentze, A. Strauch, F. Thonfeld, S.J. Zwart, A. Nelson, A new conceptual framework for integrating earth observation in large-scale wetland management in east africa, Wetlands 41 (2021) 1–21.

[45] J. Muro, A. Varea, A. Strauch, A. Guelmami, E. Fitoka, F. Thonfeld, B. Diekkrüger, B. Waske, Multitemporal optical and radar metrics for wetland mapping at national level in Albania, Heliyon 6 (2020), e04496.

[46] C.J. Weissteiner, M. Ickerott, H. Ott, M. Probeck, G. Ramminger, N. Clerici, H. Dufourmont, A.M.R. De Sousa, Europe's green arteries—a continental dataset of riparian zones, Rem. Sens. 8 (2016) 925.

[47] G.J.-P. Schumann, P.D. Bates, The need for a high-accuracy, open-access global DEM, Front. Earth Sci. 6 (2018) 225, https://doi.org/10.3389/feart.2018.00225.

[48] T.P. Higginbottom, C.D. Field, A.E. Rosenburgh, A. Wright, E. Symeonakis, S.J. Caporn, High-resolution wetness index mapping: a useful tool for regional scale wetland management, Ecol. Inf. 48 (2018) 89–96.

[49] A.E. Maxwell, T.A. Warner, Is high spatial resolution DEM data necessary for mapping palustrine wetlands? Int. J. Rem. Sens. 40 (2019) 118–137, https://doi.org/10.1080/01431161.2018.1506184.

[50] J.W. Riley, D.L. Calhoun, W.J. Barichivich, S.C. Walls, Identifying small depressional wetlands and using a topographic position index to infer hydroperiod regimes for pond-breeding amphibians, Wetlands 37 (2017) 325–338.

[51] E. Saralioglu, O. Gungor, Crowdsourcing in remote sensing: a review of applications and future directions, IEEE Geosci. Rem. Sens. Mag. 8 (2020) 89–110.

[52] P. Olofsson, G.M. Foody, M. Herold, S.V. Stehman, C.E. Woodcock, M.A. Wulder, Good practices for estimating area and assessing accuracy of land change, Rem. Sens. Environ. 148 (2014) 42–57.

[53] G.M. Foody, M. Pal, D. Rocchini, C.X. Garzon-Lopez, L. Bastin, The sensitivity of mapping methods to reference data quality: training supervised image classifications with imperfect reference data, ISPRS Int. J. Geo-Inf. 5 (2016) 199, https://doi.org/10.3390/ijgi5110199.

[54] A.C. Braun, More accurate less meaningful? A physical geographer's reflection on interpreting remote sensing land-use analyses, Prog. Phys. Geogr.: Earth Environ. (2021), https://doi.org/10.1177/0309133321991814, 0309133321991814.

[55] GBIF, GBIF, The Global Biodiversity Information Facility (Year) what Is GBIF?, 2022 (accessed March 15, 2022), https://www.gbif.org/what-is-gbif.

[56] S. Rapinel, L. Hubert-Moy, One-class classification of natural vegetation using remote sensing: a review, Rem. Sens. 13 (2021) 1892, https://doi.org/10.3390/rs13101892.

[57] D.G. Rossiter, Digital soil resource inventories: status and prospects in 2015, in: G.-L. Zhang, D. Brus, F. Liu, X.-D. Song, P. Lagacherie (Eds.), Digital Soil Mapping across Paradigms, Scales and Boundaries, Springer, Singapore, 2016, pp. 275–286, https://doi.org/10.1007/978-981-10-0415-5_22.

[58] A. Jiménez-Valverde, J.M. Lobo, Threshold criteria for conversion of probability of species presence to either–or presence–absence, Acta Oecol. 31 (2007) 361–369.

[59] N. Karasiak, J.-F. Dejoux, C. Monteil, D. Sheeren, Spatial Dependence between Training and Test Sets: Another Pitfall of Classification Accuracy Assessment in Remote Sensing, Mach Learn, 2021, https://doi.org/10.1007/s10994-021-05972-1.

[60] S.M. Chignell, M.W. Luizza, S. Skach, N.E. Young, P.H. Evangelista, An integrative modeling approach to mapping wetlands and riparian areas in a heterogeneous Rocky Mountain watershed, Rem. Sens. Ecol. Conser. 4 (2018) 150–165, https://doi.org/10.1002/rse2.63.

[61] E.A. Freeman, G.G. Moisen, A comparison of the performance of threshold criteria for binary classification in terms of predicted prevalence and kappa, Ecol. Model. 217 (2008) 48–58, https://doi.org/10.1016/j.ecolmodel.2008.05.015.

[62] Ramsar Convention Bureau, Wetlands Values and Functions, Ramsar Convention Bureau, Gland, Switzerland, 2001. https://www.ramsar.org/sites/default/files/documents/library/info2007-01-e.pdf.

[63] M. Brinson, Hydrogeomorphic Wetland Classification System: an Overview and Modification to Better Meet the Needs of the Natural Resources Conservation Service. Washington, DC, USDA, Natural Resources Conservation Service, Washington, DC, USA, 2008 accessed April 30, 2022), https://www.nrcs.usda.gov/Internet/FSE_DOCUMENTS/nrcs143_010784.pdf.

[64] J.G. Wasson, A. Chandesris, H. Pella, L. Blanc, Les hydro-écorégions : une approche fonctionnelle de la typologie des rivières pour la Directive cadre européenne sur lèau, Ingénieries - E A T, 2004, pp. 3–10.

[65] RPDZH, Réseau Partenarial des Données sur les Zones Humides, 2022 (accessed March 3, 2022), http://www.reseau-zones-humides.org/sizh.aspx.

[66] OFBObservatoireNational de la Biodiversité, 2022. https://naturefrance.fr/indicateurs/evolution-de-letat-general-des-zones-humides. (Accessed 15 March 2022). accessed.

[67] E. Grolleau, L. Bargeot, A. Chafchafi, R. Hardy, J. Doux, A. Beaudou, H.L. Martret, J.C. Lacassin, J.L. Fort, P. Falipou, D. Arrouays, Le système d'information national sur les sols: DONESOL et les outils associés, Étude Gestion Sols 11 (2004) 255.

[68] U. Infosol, DoneSol: la base de données nationale des sols de France, in: Conférence Année Internationale Des Sols, AIS), 2015.

[69] J.-C. Hervé France, C. Vidal, I.A. Alberdi, L. Hernández Mateo, in: J.J. Redmond (Ed.), National Forest Inventories: Assessment of Wood Availability and Use, Springer International Publishing, Cham, 2016, pp. 385–404, https://doi.org/10.1007/978-3-319-44015-6_20.

[70] L. Poncet, La diffusion de l'information sur la biodiversité en France. L'exemple de l'inventaire national du patrimoine naturel (INPN), Netcom. Réseaux, Communication et Territoires (2013) 181–189.

[71] G. Barnaud, E. Fustec, Conserver les zones humides : pourquoi ? comment ? Editions Quae, 2007.

[72] P. Mérot, P. Curmi, A. Laplace-Dolonde, Les sols des zones humides, MEDD, Agences de l'eau, BRGM, 2005.

[73] R.W. Tiner, Wetland Indicators: A Guide to Wetland Formation, Identification, Delineation, Classification, and Mapping, CRC press, 2016.

[74] H. Ellenberg, H.E. Weber, R. DULL, V. Wirth, Zeigerwerte von Pflanzen in Mitteleuropa, E. Goltze, 1991.

[75] P.H. Julve, Baseflor. Index botanique, écologique et chorologique de la flore de France, Institut Catholique de Lille, Lille, 1998.

[76] J.B. Bouzillé, Écologie des zones humides, Concepts, Méthodes et Démarches, Tec & Doc-Lavoisier, Paris, 2014.

[77] J. Inglada, A. Vincent, M. Arias, B. Tardy, D. Morin, I. Rodes, Operational high resolution land cover map production at the country scale using satellite image time series, Rem. Sens. 9 (2017) 95.

[78] C.E. Davies, D. Moss, M.O. Hill, EUNIS Habitat Classification Revised 2004, Report to, European Environment Agency-European Topic Centre on Nature Protection and Biodiversity, 2004, pp. 127–143.

[79] G. Gayet, F. Botcazou, J.-M. Gibeault-Rousseau, L. Hubert-Moy, S. Rapinel, B. Lemercier, Field dataset of punctual observations of soil properties and vegetation types distributed along soil moisture gradients in France, Data Brief 45 (2022), 108632, https://doi.org/10.1016/j.dib.2022.108632.

[80] IGN, RGE ALTI - Le modèle numérique de terrain (MNT) maillé qui décrit le relief du territoire français à grande échelle, Geoservices, 2021 (accessed March 7, 2022), https://geoservices.ign.fr/rgealti#telechargement5m.

[81] M.D. Correll, W. Hantson, T.P. Hodgman, B.B. Cline, C.S. Elphick, W.G. Shriver, E.L. Tymkiw, B.J. Olsen, Fine-scale mapping of coastal plant communities in the northeastern USA, Wetlands (2018) 1–12.

[82] S. Rapinel, J.-B. Bouzillé, J. Oszwald, A. Bonis, Use of bi-seasonal landsat-8 imagery for mapping marshland plant community combinations at the regional scale, Wetlands 35 (2015) 1043–1054, https://doi.org/10.1007/s13157-015-0693-8.

[83] K. Beven, M. Kirkby, A physically based, variable contributing area model of basin hydrology, Hydrol. Sci. Bull. 24 (1979) 43–69.

[84] T.G. Freeman, Calculating catchment area with divergent flow based on a regular grid, Comput. Geosci. 17 (1991) 413–422, https://doi.org/10.1016/0098-3004(91)90048-I.

[85] M. Kopecký, Š. Čížková, Using topographic wetness index in vegetation ecology: does the algorithm matter? Appl. Veg. Sci. 13 (2010) 450–459.

[86] I.G.N. OFB, BD TOPAGE, Service d'administration nationale des données et référentiels sur l'eau, 2022. https://www.sandre.eaufrance.fr/atlas/srv/eng/catalog.search#/metadata/7fa4c224-fe38-4e2c-846d-dcc2fa7ef73e.

[87] S. Rapinel, B. Clément, S. Dufour, L. Hubert-Moy, Fine-scale monitoring of long-term wetland loss using LiDAR data and historical aerial Photographs, the Example of the Couesnon Floodplain, France, Wetlands 38 (2018) 423–435.

[88] J.B. Lindsay, J.M.H. Cockburn, H.A.J. Russell, An integral image approach to performing multi-scale topographic position analysis, Geomorphology 245 (2015) 51–61.

[89] BRGM, BD-CHARM, Geological Map at 1:50 000, InfoTerre, 2022 (accessed March 7, 2022), http://infoterre.brgm.fr/formulaire/telechargement-cartes-geologiques-departementales-150-000-bd-charm-50.

[90] C. Seger, An Investigation of Categorical Variable Encoding Techniques in Machine Learning: Binary versus One-Hot and Feature Hashing, 2018.

[91] R. Valavi, J. Elith, J.J. Lahoz-Monfort, G. Guillera-Arroita, blockCV, An r package for generating spatially or environmentally separated folds for k-fold cross-validation of species distribution models, Methods Ecol. Evol. 10 (2019) 225–232, https://doi.org/10.1111/2041-210X.13107.

[92] L. Breiman, Random forests, Mach. Learn. 45 (2001) 5–32, https://doi.org/10.1023/A:1010933404324.

[93] M. Belgiu, L. Drăguţ, Random forest in remote sensing: a review of applications and future directions, ISPRS J. Photogrammetry Remote Sens. 114 (2016) 24–31.

[94] H.R. Sofaer, J.A. Hoeting, C.S. Jarnevich, The area under the precision-recall curve as a performance metric for rare binary events, Methods Ecol. Evol. 10 (2019) 565–577, https://doi.org/10.1111/2041-210X.13140.

[95] M. Kuhn, K. Johnson, Applied Predictive Modeling, Springer-Verlag, New York, NY, USA, 2013.

[96] M. Kuhn, Caret package, J. Stat. Software 28 (2008) 1–26.

[97] R.J. Hijmans, R. Bivand, J. van Etten, K. Forner, J. Ooms, E. Pebesma, Package 'terra, 2022.

[98] A. Brenning, D. Bangs, M. Becker, P. Schratz, F. Polakowski, Package 'RSAGA,' The Comprehensive R Archive Network, 2018. https://CRAN-R-Project.Org/Package=RSAGA. Accessed on 31 January 2023.

[99] J.B. Lindsay, G.A.T. Whitebox, A case study in geomorphometric analysis, Comput. Geosci. 95 (2016) 75–84, https://doi.org/10.1016/j.cageo.2016.07.003.

[100] R. Bivand, T. Keitt, B. Rowlingson, Rgdal: Bindings for the Geospatial Data Abstraction Library, 2015. http://CRAN.R-project.org/package=rgdal.

[101] QGIS Development Team, QGIS Version 2.18. 22, Geographic Information System, 2018.

[102] I. Jarić, F. Quétier, Y. Meinard, Procrustean beds and empty boxes: on the magic of creating environmental data, Biol. Conserv. 237 (2019) 248–252.

[103] H.A. Ullerud, A. Bryn, R. Halvorsen, L.Ø. Hemsing, Consistency in land-cover mapping: influence of field workers, spatial scale and classification system, Appl. Veg. Sci. 21 (2018) 278–288.

[104] V. Rodriguez-Galiano, B. Ghimire, J. Rogan, M. Chica-Olmo, J.P. Rigol-Sanchez, An assessment of the effectiveness of a random forest classifier for land-cover classification, ISPRS J. Photogrammetry Remote Sens. 67 (2012) 93–104.

[105] I. Burdun, M. Bechtold, V. Sagris, V. Komisarenko, G. De Lannoy, Ü. Mander, A comparison of three trapezoid models using optical and thermal satellite imagery for water table depth monitoring in Estonian bogs, Rem. Sens. 12 (2020) 1980, https://doi.org/10.3390/rs12121980.

[106] G. Kaplan, U. Avdan, G. Kaplan, U. Avdan, Monthly analysis of wetlands dynamics using remote sensing data, ISPRS Int. J. Geo-Inf. 7 (2018) 411, https://doi.org/10.3390/ijgi7100411.

[107] S.V. Stehman, G.M. Foody, Key issues in rigorous accuracy assessment of land cover products, Rem. Sens. Environ. 231 (2019), 111199, https://doi.org/10.1016/j.rse.2019.05.018.

[108] L. Chasmer, C. Mahoney, K. Millard, K. Nelson, D. Peters, M. Merchant, C. Hopkinson, B. Brisco, O. Niemann, J. Montgomery, K. Devito, D. Cobbaert, Remote sensing of boreal wetlands 2: methods for evaluating boreal wetland ecosystem state and drivers of change, Rem. Sens. 12 (2020) 1321, https://doi.org/10.3390/rs12081321.

[109] M.A. Günen, Performance comparison of deep learning and machine learning methods in determining wetland water areas using EuroSAT dataset, Environ. Sci. Pollut. Control Ser. (2021) 1–15.

[110] B. Hosseiny, M. Mahdianpari, B. Brisco, F. Mohammadimanesh, B. Salehi, WetNet: a spatial-temporal ensemble deep learning model for wetland classification using sentinel-1 and sentinel-2, IEEE Trans. Geosci. Rem. Sens. (2021).

[111] S. López-Tapia, P. Ruiz, M. Smith, J. Matthews, B. Zercher, L. Sydorenko, N. Varia, Y. Jin, M. Wang, J.B. Dunn, Machine learning with high-resolution aerial imagery and data fusion to improve and automate the detection of wetlands, Int. J. Appl. Earth Obs. Geoinf. 105 (2021), 102581.

[112] N.A. Rivers-Moore, D.C. Kotze, N. Job, S. Mohanlal, Prediction of wetland hydrogeomorphic type using morphometrics and landscape characteristics, Front. Environ. Sci. 8 (2020) (accessed March 28, 2022), https://www.frontiersin.org/article/10.3389/fenvs.2020.00058.

[113] G. Büttner, G. Maucha, B. Kosztra, High-Resolution Layers, European Landscape Dynamics: CORINE Land Cover Data, 2016, p. 61.

[114] Z.S. Venter, M.A.K. Sydenham, Continental-scale land cover mapping at 10 m resolution over Europe (ELC10), Rem. Sens. 13 (2021) 2301, https://doi.org/10.3390/rs13122301.

[115] M. Buchhorn, B. Smets, L. Bertels, B.D. Roo, M. Lesiv, N.-E. Tsendbazar, M. Herold, S. Fritz, Copernicus Global Land Service: Land Cover 100m: Collection 3: Epoch 2019, Globe, 2020, https://doi.org/10.5281/zenodo.3939050.

[116] Ramsar Convention on Wetlands, Scaling up Wetland Conservation, Wise Use and Restoration to Achieve the Sustainable Development Goals 2018, 2015. https://ramsar.org/sites/default/files/documents/library/cop12_res02_strategic_plan_e_0.pdf.

[117] C.B.D. Secretariat, The strategic plan for biodiversity 2011–2020 and the Aichi biodiversity targets, in: Secretariat of the Convention on Biological Diversity, Nagoya, Japan, 2010.

[118] United Nations, Transforming Our World: The 2030 agenda For sustainable Development, Outcome Document for the UN Summit to Adopt the Post-2015 Development Agenda, New York, NY, USA, 2015.

[119] J.E. Viñuales, The Paris agreement on climate change, German YB Int'l L. 59 (2016) 11.

[120] G. Kallis, D. Butler, The EU water framework directive: measures and implications, Water Pol. 3 (2001) 125–142.

[121] Council Directive 92/43/EEC, Conservation of natural habitats and of wild flora and fauna, L206, Int. J. Eur. Comm. (1992) 7–49.

[122] INPN, The National Map of the Biodiversity Cores and the Corridors, 2017. https://inpn.mnhn.fr/programme/trame-verte-et-bleue/carte-nationale?lg=en.

[123] MTECT, Plan biodiversité, 2021. https://www.ecologie.gouv.fr/plan-biodiversite.

[124] P. Puydarieux, W. Beyou, L'Évaluation Française des Écosystèmes et des Services Écosystémique—Cadre Conceptuel, Ministère de l'Environnement & Fondation Pour La Recherche Sur La Biodiversité, 2017.

[125] E.E.A. CLMS, High Resolution Land Cover Characteristics - Lot 4: Water & Wetness 2018, Copernicus Land Monitoring Service, 2020.